The pH Dependence of the Spectral and Anion Binding Properties of Iron Containing Superoxide Dismutase from *E. Coli* B: An Explanation for the Azide Inhibition of Dismutase Activity*

JAMES A. FEE,[a,**] GREGORY J. MCCLUNE,[a,†] ALISON C. LEES,[a] RAPHAEL ZIDOVETZKI [b] AND ISRAEL PECHT[b]

[a]Biophysics Research Division and the Department of Biological Chemistry, The University of Michigan, Ann Arbor, MI, USA; and [b]Department of Chemical Immunology, The Weizmann Institute of Science, Rehovot, Israel

(*Received 20 May 1980*)

Abstract. Examination of the optical and EPR properties of the ferric form of the iron containing superoxide dismutase from *E. coli* B, at pH values ranging from 4.5 to 10.9, has revealed two reversible structural transitions affecting the Fe^{3+} ion. The apparent pK_a values of these transitions are 5.1 ± 0.3 and 9.0 ± 0.3. The binding of azide has been studied over the pH range 4.5 to 10.7; the affinity of the Fe^{3+} for N_3^- is independent of pH from 4.5 to ~7.5, after which the dissociation constant decreased by a factor of 10 per unit increase in pH. The apparent pK_a which affects N_3^- binding to the iron is 8.6 ± 0.2. The association of N_3^- with the iron has been examined using the temperature-jump method at pH 7.4 and 9.3. The kinetics of ligand association were shown to conform to the minimal mechanism:

$$P\text{-}Fe^{3+} + N_3^- \overset{K_1}{\rightleftharpoons} N_3^-\text{-}P\text{-}Fe^{3+} \overset{K_2}{\rightleftharpoons} P\text{-}Fe^{3+}\text{-}N_3^-.$$

K_1 was found to be essentially unaffected by pH whereas K_2 was much lower at pH 9.3 than at 7.4. The value of K_1 at pH 7.4 (100 M^{-1}) corresponds very closely to that obtained for the inhibition constant of azide, 10 mM.[12] A scheme is presented in which N_3^- inhibits the iron containing dismutase by competing with O_2^- for an anion binding site near, but not on the Fe^{3+}.

INTRODUCTION

The iron containing superoxide dismutases were first discovered by Yost and Fridovich[1] and subsequently shown to be present in a variety of microorganisms including strict anaerobes.[2-8]

These proteins consist of two identical subunits having a molecular weight of ~38,000 with each apparently binding a single Fe^{3+}.[3,9] Nuclear magnetic relaxation studies by Villafranca[10,11] have shown that at least one water molecule is associated with the ferric ion. Slykhouse and Fee[9] examined the spectral properties of the protein from *E. coli* B, observed that F^- and N_3^- could bind to the Fe^{3+} and noted an unusual discrepancy between the affinity of the Fe^{3+} for these anions and their ability to inhibit the dismutase activity. Thus, spectral measurements showed that these anions had dissociation constants of 1–2 mM, but inhibition constants of 30–50 mM[9,12] for F^- and ~10 mM for N_3^-.[12] The purposes of this communication are to describe the pH dependence of the spectral properties of the bound Fe^{3+} and its association with N_3^- and to offer a tentative explanation for the disparity in the binding constants of anions to Fe^{3+} and their ability to inhibit the dismutase activity.

MATERIALS AND METHODS

Iron containing superoxide dismutase was purified from *E. coli* B cell paste (Grain Products, Muscatine, Iowa), according to the method of Slykhouse and Fee.[9] All other substances were of the highest commercial quality available and glass distilled water was used throughout.

Optical measurements were made with a Zeiss DMR-21 recording spectrophotometer and EPR spectra were recorded at cryogenic temperatures using a Varian E-112 spectrometer.

Kinetic measurements were done on a temperature jump spectrofluorometer[13] operating in the absorption mode. A capacitor discharge of 20kV raised the temperature of the solution by 5.2 °C from 2 ± 0.1 °C, in approximately 1 μsec. The absorption changes were monitored at 440 nm. The signals were fed into a Biomation 802 transient recorder (Biomation, Cupertino, CA). At each concentration, the sum of several relaxation curves was recorded on magnetic tape using a recorder operated by a Hewlett–Packard 2100 mini-computer and then was transferred to an IBM 370/165 computer for detailed analysis. The curves were fitted to a sum of exponents using a modified Marquart algorithm.[14] The quality of the fit was determined from the deviation between the experimental data and the simulated curve, as well as from the auto-correlation function.[15] Figure 6 shows a sample analysis. The experimental concentration dependences of the relaxation times and amplitudes were fitted to expressions derived according to Castellan[16] and Jovin[17] for the specific reaction mechanism (see the section below entitled "Results"). The fitting was done using a NAG library subroutine which allows placement of constraints on parameters and their functions.[16] Application of this program yields a complete set of kinetic and thermodynamic parameters for a given reaction mechanism.

RESULTS

The variation of the EPR spectra of iron dismutase in the pH range 4 to 11 is shown in Fig. 1. The unique g 4.3

* Supported by U.S.P.H.S. research grant GM 21519 (J.A.F.).

** Address all inquiries to this author at the Biophysics Research Division, 2200 Bonisteel Blvd., Ann Arbor, MI 48109 USA.

† Present address: Inorganic Chemistry Laboratory, Oxford University, Oxford, England.

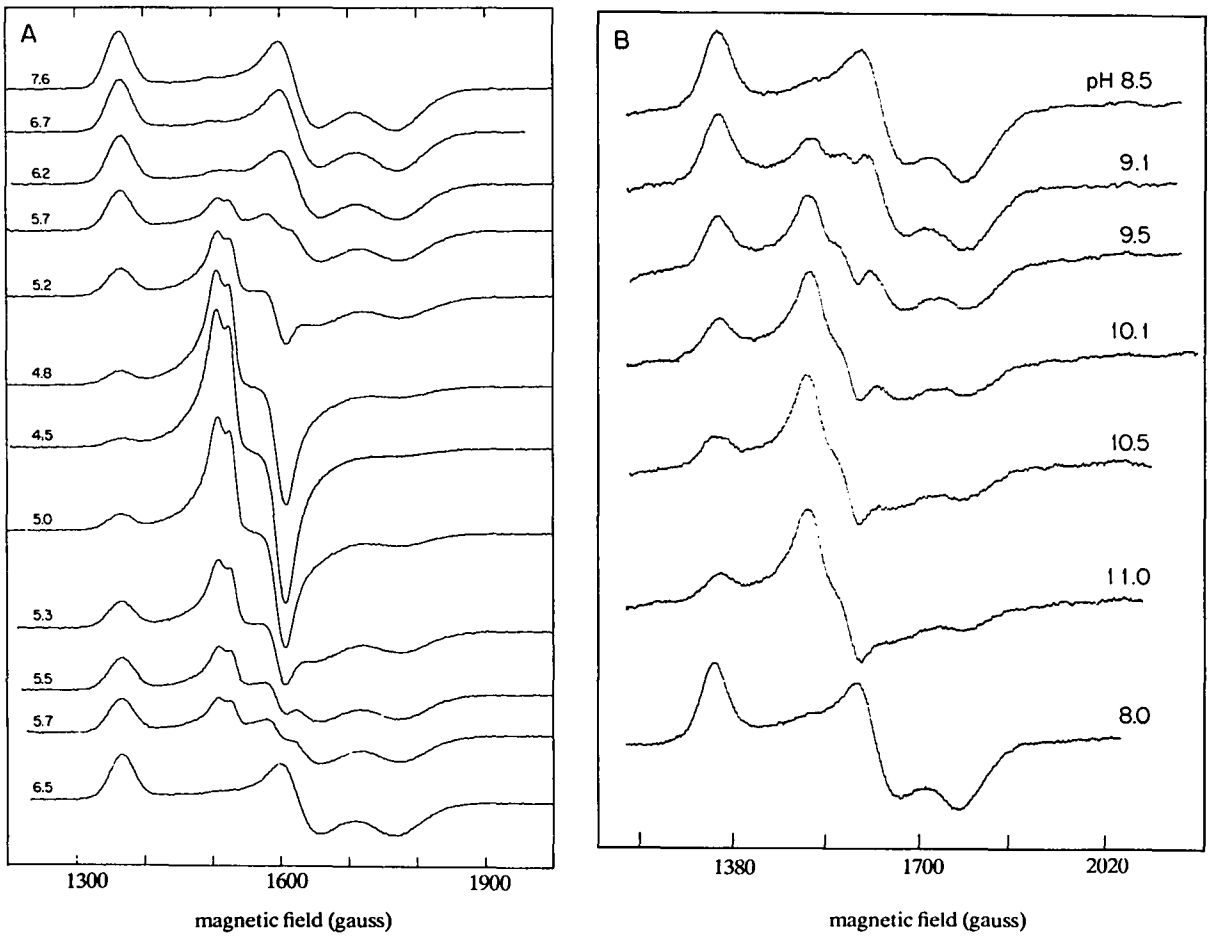

Fig. 1. The effect of low pH (Panel A) and high pH (Panel B) on the EPR spectrum of iron containing superoxide dismutase from *E. coli* B. The spectra were recorded at 100°K, microwave frequency ~9.2, modulation frequency = 100 kHz, modulation amplitude = 10 gauss, sweep time was 250 gauss/min. The concentration of Fe as iron protein was ~0.25 mM, and the pH was adjusted by adding 1 M HCl or NaOH to a rapidly stirred solution. Great care had to be taken at lower pH to avoid locally high concentrations of acid which led to irreversible precipitation at the protein. Undoubtedly this accounted for some irreversibility.

signal of the Fe^{3+} gives way to different signals at pH values above and below neutrality. These effects are largely reversible in the high pH region but to a lesser extent in the low pH region. Virtually no optical changes beyond a bleaching due to irreversible denaturation are observed at low pH (not shown), but at high pH a reversible bleaching of the 350 nm band is observed (Fig. 2). Changes in both the optical and EPR spectra are expressed in Fig. 3 as the percent of native (or neutral) signal present over the pH range 4 to 11. The apparent pK_a values assigned to these transitions are 5.1 ± 0.1 and 9 ± 0.3.*

As shown earlier,[9] when N_3^- binds to the iron, a broad absorption band develops at 440 nm. A typical optical titration of the iron dismutase with N_3^- is shown in Fig. 4; the inset shows the inverse plot from which dissociation constants were typically obtained. Such experiments have been conducted over a wide pH range at constant ionic strength and temperature. The logarithm of the dissociation constant of N_3^- is plotted in Fig. 5. The data were fitted using a non-linear least squares program to the expression

$$K_d = K_{d_0}(1 + 10^{(pH - pK_a)}) \quad (1)$$

in which the best fit yielded $pK_a = 8.6 \pm 0.3$. The inset of Fig. 5 is a plot of $\ln K_a$ vs. $1/T°$ K, in which the temperature was varied from 5°C to 40°C. The thermodynamic parameters of association at pH 7.4 calculated from these data were $\Delta H = -8.3$ kcal/mol and $\Delta S = 15.3$ cal/mol-deg.

The substantial enthalpy associated with the binding of azide suggested that the temperature-jump method may yield valuable information about the mechanism of anion binding. Therefore, the binding of N_3^- was examined by this method. Figure 6 shows a typical time dependence of the absorbance at 440 nm upon raising the temperature of a solution of Fe^{3+}–superoxide dismutase and N_3^- from 2° to 7.2°C. A single exponential was observed under all conditions of measurement. The concentration dependence of the reciprocal relaxation times is given in Fig. 7.

* At present we have no explanation for the large amount of scatter in the data presented in Fig. 3. Each transition appears to exhibit a certain amount of kinetic restraint, and since the data were assembled from several independent measurements, it is possible that final equilibrium was not achieved in all cases.

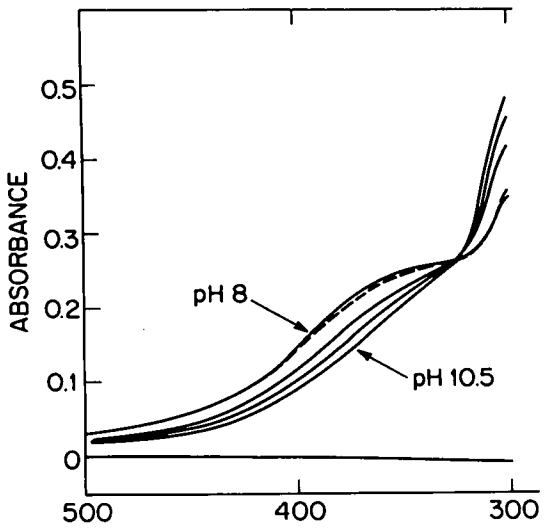

Fig. 2. The effect of high pH on the optical spectrum of iron containing superoxide dismutase from *E. coli* B. The dashed line denotes readjustment of the sample from pH 10.5 to 8. Some precipitation occurs during these experiments and it is necessary to centrifuge the sample after each adjustment of the pH.

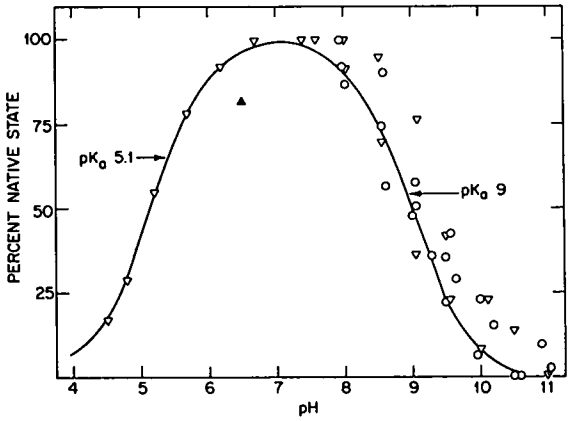

Fig. 3. Dependence of the neutral form of iron superoxide dismutase from *E coli* B over the pH range 4.5 to 10.9. The circles indicate optical changes as shown in Fig. 2 and the triangles relative changes in the EPR spectrum from Fig. 1. ▲ indicates reversibility from low pH.

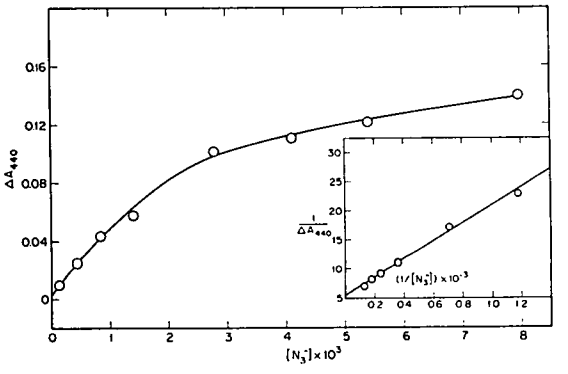

Fig. 4. Optical titration of Fe^{3+} superoxide dismutase from *E. coli* B with NaN_3. The protein solution was buffered with 25 mM $Na_2P_2O_7$ at pH 8.7. Temp. = 25 °C, ionic strength = 0.25, Fe = 0.19 mM, pathlength = 1 cm. *Inset*: Plot of A_{440}^{-1} vs. $[N_3^-]^{-1}$. K_d was obtained by dividing the slope of this line by its intercept at $[N_3^-]^{-1} = 0$.

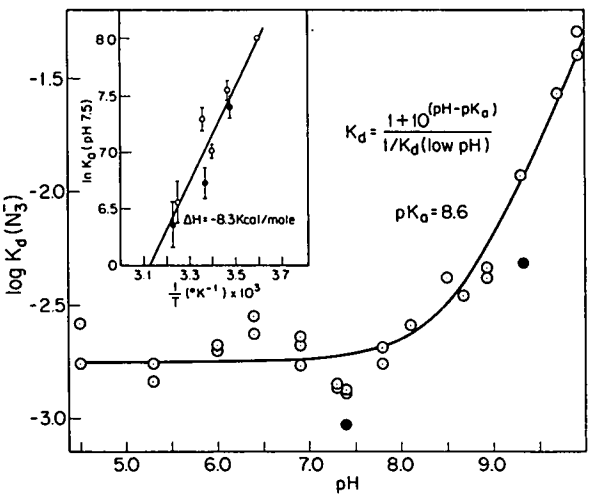

Fig. 5. The dissociation constant for the binding of N_3^- to ferri superoxide dismutase from *E. coli* B at 25 °C as a function of pH. The concentration of N_3^- was calculated from $[NaN_3]_{tot}(K_a/(H^+ + K_a))$ using $pK_a = 4.6$.[23] *Inset*: Arrhenius plot of the association constant. (Symbols including an "×" were taken from experiments in which 10% glycerol was included in the protein solution. All experiments were done at ionic strength = 0.25).

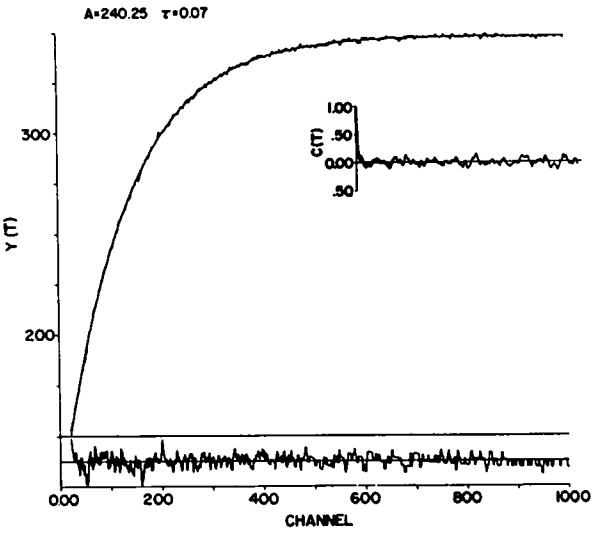

Fig. 6. Example of the analysis and fitting of the *T*-jump relaxation curves monitored via 440 nm absorption changes. P–Fe^{3+} concentration was 3.55×10^{-4} M and N_3^- concentration was 3.98×10^{-3} M. The presented data are a sum of 2 independent *T*-jumps. The ordinate shown digitized Biomation units and the abscissa the channel number of the Biomation memory. The sampling rate was 0.5 ms per 1000 channels. The data are fitted to one exponent and the resulting amplitude (A, in mV) and relaxation time (τ, in ms) are presented. The solid line is drawn using these parameters. The total signal after the jump was 8000 mV. Insert, top right, is the auto-correlation analysis of the fit. The lower part shows the deviation between experimental and fitted curves, normalized to the largest deviation. Additional details are in Materials and Methods.

It can be seen that $1/\tau$ does not increase linearly, as would be expected for a bimolecular association, but levels off with increasing concentration of N_3^-. This behavior is consistent with the presence of a fast bimolecular association, together with a slower monomolecular step, where only the latter contributes to the absorption change. The formulae describing this mechanism are given in Ref. 19 (mechanism 1, slow time, slow amplitude). The fit obtained using this mechanism for the concentration dependencies of the reciprocal relaxation times (Fig. 7) and the amplitudes of the absorption change (Fig. 8) shows a good agreement with the experimental data. The kinetic and thermodynamic parameters obtained as a result of the fitting procedure are summarized in Table 1. When comparable, the parameters obtained from the analysis of the kinetic data are in good agreement with those obtained from equilibrium measurements (cf. solid symbols in Fig. 5).

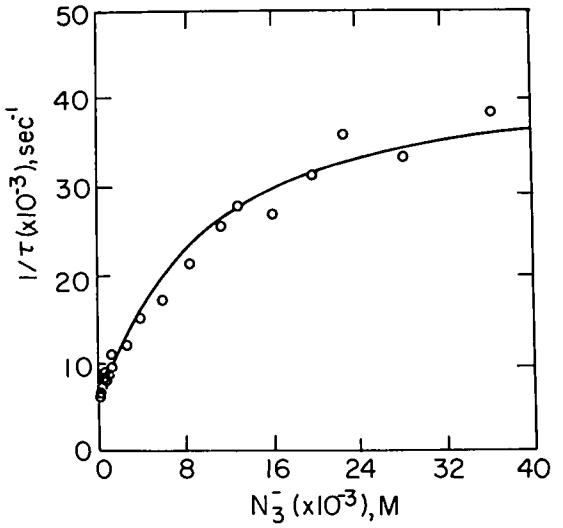

Fig. 7. The dependence of the reciprocal relaxation times on total N_3^- concentration at 7.2 °C. Initial P-Fe^{3+} concentration is 3.7×10^{-4} M.

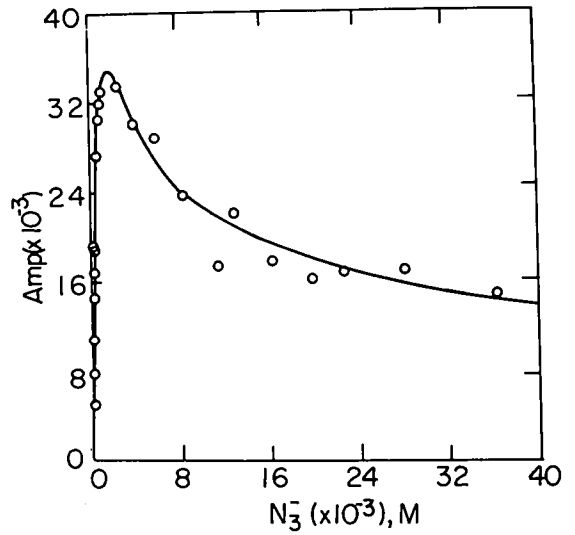

Fig. 8. The dependence of relaxation amplitudes on total N_3^- concentration at 7.2 °C. Initial P-Fe^{3+} concentration is 3.7×10^{-4} M.

Table 1. Kinetic and Thermodynamic Parameters Obtained from Temperature Jump Studies of the Binding of Azide to Iron Superoxide Dismutase from *E. Coli* B*

pH	7.4	9.3
$K_{overall}$ (M^{-1})	940	190
K_1 (M^{-1})	107	66
K_2 (M^{-1})	7.7	1.9
k_2 (s^{-1})	3.9×10^5	1.0×10^4
k_{-2} (s^{-1})	5.0×10^3	5.2×10^3
$\Delta H_{overall}$ (kcal/mol)	−5.3	−3.6
ΔH_1 (kcal/mol)	−0.1	−1.4
ΔH_2 (kcal/mol)	−5.9	−3.3
$\Delta\varepsilon_{overall}$ ($M^{-1}cm^{-1}$)	1100	1200
$\Delta\varepsilon_2$ ($M^{-1}cm^{-1}$)	1240	1820

We estimated the error by simulations and parameter variation as ± 15%. The protein was dissolved in 0.15 M NaCl, 0.02 M sodium phosphate. a. The primary data were fit to the scheme

$$N_3^- + P\text{-}Fe^{3+} \underset{K_1}{\rightleftharpoons} N_3^-P\text{-}Fe^{3+} \underset{K_2}{\rightleftharpoons} P\text{-}Fe^{3+} - N_3^-$$

DISCUSSION

The spectral changes indicate modifications of structure in the region of the Fe^{3+} slightly above and below neutrality. The following suggestions are made in the explanation of these changes. Because there is no change in the optical spectrum at low pH, we suggest that the atoms liganding to the Fe^{3+} are not protonated, but rather that a general conformational change of the protein leads to a modification of the ligand field parameters, which accounts for the unusual rhombicity of this signal as expressed by the presence of three apparent g-values centered around $g = 4.27$[20] in the native protein. This idea is also supported by the observation that the affinity of the Fe^{3+} for N_3^- is not affected in this pH region.

The transition at high pH is considered to involve the hydrolysis of a metal bound water molecule:[11]

$$P\text{-}Fe^{3+}\text{-}OH_2 \rightarrow P\text{-}Fe^{3+}\text{-}OH^- + H^+. \quad (2)$$

The decrease in long wavelength absorption is consistent with introducing a less polarizable, negatively charged ligand atom into the coordination sphere, thus forcing the metal to ligand charge transfer band (s) toward the ultraviolet as occurs when F^- associates with the Fe^{3+}.[9] Except to show that the Fe^{3+} remains high spin, little can be said of the observed EPR changes.

In contrast to the low pH transition, which does not affect the affinity of the Fe^{3+} for N_3^-, the high pH form of the protein clearly has a lower affinity for this anion. The data are consistent with the following equilibria:

$$Fe^{3+}\text{-}OH_2 + N_3^- \rightleftharpoons Fe^{3+}\text{-}N_3^- + H_2O \quad (3)$$

$$Fe^{3+}\text{-}OH_2 \rightleftharpoons Fe^{3+}\text{-}OH^- + H^+. \quad (4)$$

Analysis of the data within this formalism (cf Expression (1)) yields a value for $pK_a = 8.6 \pm 0.3$. While this value appears to be slightly lower than that obtained from the spectroscopic observations, the evident scatter in the data precludes the idea that different ionization processes are affecting the N_3^- binding and the spectral properties of the Fe^{3+}.* Our present interpretation of the high pH data is that the factors causing the spectral changes at high pH are also decreasing the affinity of the Fe^{3+} for N_3^-,

* Thus, the pK_a of 9.3 + 0.3 (Fig. 3) is tentatively considered not to differ from pK_a 8.6 + 0.3 (Fig. 5); more precise data may yield a distinction.

as expressed in Reactions (2) and (3) from which (1) is derived.

One of the intriguing aspects of this enzyme is the large discrepancy in the affinity of anions for the Fe^{3+} form and their ability to inhibit the catalysis of superoxide dismutation. A summary of these constants is presented in Table 2. As previously reported,[9] the Fe^{3+} form of this protein has very unusual anion binding properties. Thus, CN^- did not appear to bind at any readily attainable concentration, while F^- and N_3^- produced spectral changes with apparent dissociation constants of 1–2 mM. One of the puzzling features of these annation reactions was that they did not lead to inhibition of catalysis. Thus, as shown in Table 2, a 10–20-fold higher concentration was found to be required to give half-inhibition than was required to give half-saturation of the Fe^{3+} form of the protein, as indicated by spectral measurements. Moreover, we have found that ClO_4^-, which is an extremely poor ligand for the metal ions,[21] is a competitive inhibitor of catalysis (G. J. McClune and J. A. Fee, unpublished observations); this led to the idea that anions, in addition to directly coordinating the Fe^{3+}, may also bind near but not directly to the Fe^{3+}. Perchlorate, which inhibits half the dismutase activity at ~20 mM, effects only a minor perturbation in the EPR spectrum at this concentration; it clearly does not bind to the metal.

Table 2. Comparison of the Dissociation and Inhibition Constants of F^- and N_3^- for the Iron Superoxide Dismutase of *E. coli* B at pH 7.4

	F	N_3	ClO_4^-
K_d(mM)	1–2[a]	1–2[a]	
K_i(mM)	30–50[a,b]	~10[b,c]	~20[d]

a. Ref. 9. b. Ref. 12. c. Ref. 22. These authors report a somewhat lower concentration (4–5 mM) of azide required to give 50% inhibition. However, due to the complexity of the assay media used[9] these values cannot be considered as inhibition constants. d. G. J. McClune and J. A. Fee, unpublished.

In order to account for the inhibition by ClO_4^- and to offer an explanation for the discrepancy between the dissociation and the competitive inhibition constants presented in Table 2, it is proposed that an anion binding pocket exists near the Fe^{3+} (Scheme 1) which is important in the catalytic process.

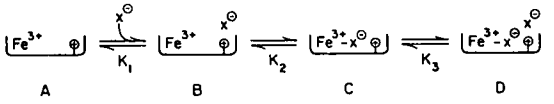

Scheme 1

The temperature-jump data assembled in Table 1 are consistently interpreted in terms of the first two equilibria of Scheme 1, in which N_3^- first associates with the protein in a second order process to form a complex having optical absorption at 440 nm indistinguishable from that of the native protein. This step is followed by a first-order process to yield the annated Fe^{3+}. The presence of the third equilibrium would only be detected by this method if it was attended by additional spectral changes and it was slower than the other reactions. The data of Table 1 can be rationalized in terms of the above scheme. The pH dependence of the overall K is due primarily to changes in K_2, while K_1 is essentially independent of pH. This is consistent with the OH^- being a more favorable ligand to Fe^{3+} at pH 9.3 than 7.4. It will be noted that the value of K_1 corresponds quite closely with the observed competitive inhibition constant for N_3^- under quite similar conditions. This, and the fact that no spectral change can be associated with K_1, leads us to suggest that competitive inhibition of catalytic activity is due to the binding of N_3^- (and other anions) in the pocket as depicted in Scheme 1.

The proposed mechanism of inhibition has several implications for the mechanism of catalysis of superoxide dismutation. Thus, in Scheme 1 the A and C forms must be able to participate essentially unhindered. This would be true if electron transfer were to occur from O_2^- bound in the pocket to Fe^{3+}–X^- at equal rates, a testable hypothesis. Further, forms B and D would be inactive because of the exclusion of O_2^- from the anion binding pocket. These ideas will be further discussed in a forthcoming communication concerned with the detailed mechanism of catalysis (Fee et al., in preparation).

REFERENCES

1. F. J. Yost, Jr. and I. Fridovich, *J. Biol. Chem.*, **248**, 4905 (1973).
2. K. Puget and A. M. Michelson, *Biochimie*, **56**, 1255 (1974).
3. K. Asada, K. Yoshikawa, M. Takahashi, Y. Maeda and K. Enmanji, *J. Biol. Chem.*, **250**, 2801 (1975).
4. E. Kusnnose, K. Ichihara, Y. Noda and M. Kusunose, *J. Biochem., (Tokyo)*, **80**, 1343 (1976).
5. F. Yamakura, *Biochim. Biophys. Acta*, **422**, 280 (1976).
6. E. C. Hatchikan and Y. A. Henry, *Biochimie*, **59**, 153 (1977).
7. S. Kanematsu and K. Asada, *FEBS Lett.*, **91**, 94 (1978).
8. S. Kanamatsu and K. Asada, *Arch. Biochem. Biophys.*, **185**, 473 (1978).
9. T. O. Slykhouse and J. A. Fee, *J. Biol. Chem.*, **251**, 5472 (1976).
10. J. J. Villafranca, F. J. Yost, Jr. and I. Fridovich, *J. Biol. Chem.*, **249**, 3532 (1974).
11. J. J. Villafranca, *FEBS Lett.*, **62**, 230 (1976).
12. J. A. Fee and G. J. McClune in T. P. Singer and R. N. Ondarza, eds., *Mechanisms of Oxidizing Enzymes*, Elsevier/North Holland, 1978, pp. 273–284.
13. R. Rigler, C. R. Rabl and T. M. Jovin, *Rev. Sci. Instrum.*, **45**, 580 (1974).
14. R. Fletcher in Harwell Subroutine Library, Atomic Energy Research Establishment, Harwell, U.K. (Subroutine VB01A) (1971).
15. A. Grinvald and I. Z. Steinberg, *Anal. Biochem.*, **59**, 583 (1974).
16. G. W. Castellan, *Ber. Bunsenges. Phys. Chem.*, **67**, 898 (1963).
17. T. M. Jovin in R. F. Chen and H. Edelhoch, eds., *Biochemical Fluorescence Concepts*, Vol. 1, Marcel Dekker, New York, 1975, pp. 305–374.
18. D. E. Gill and W. Murray in NAG Fortran Library from the Numerical Algorithms Group of Oxford University, Mark 6 (Subroutine E04UAF) (1978).
19. D. Lancet and I. Pecht, *Proc. Natl. Acad. Sci. U.S.A.*, **73**, 3549 (1976).
20. R. Aasa, *J. Chem. Phys.*, **52**, 3919 (1970).
21. F. A. Cotton and G. Wilkinson, *Advanced Inorganic Chemistry*, Interscience Publishers, New York, 1962, pp. 449–450.
22. H. P. Misra and I. Fridovich, *Arch. Biochem. Biophys.*, **189**, 317 (1978).
23. D. Seewald and N. Sutin, *Inorg. Chem.*, **2**, 643 (1963) and references therein.